^{1}H, ^{13}C, and ^{15}N backbone and side chain chemical shift assignment of YdaS, a monomeric member of the HigA family

Maruša Prolič-Kalinšek, Pieter De Bruyn, Dukas Jurėnas, Laurence Van Melderen, Remy Loris & Alexander N. Volkov

Biomolecular NMR Assignments

ISSN 1874-2718

Biomol NMR Assign
DOI 10.1007/s12104-019-09915-9

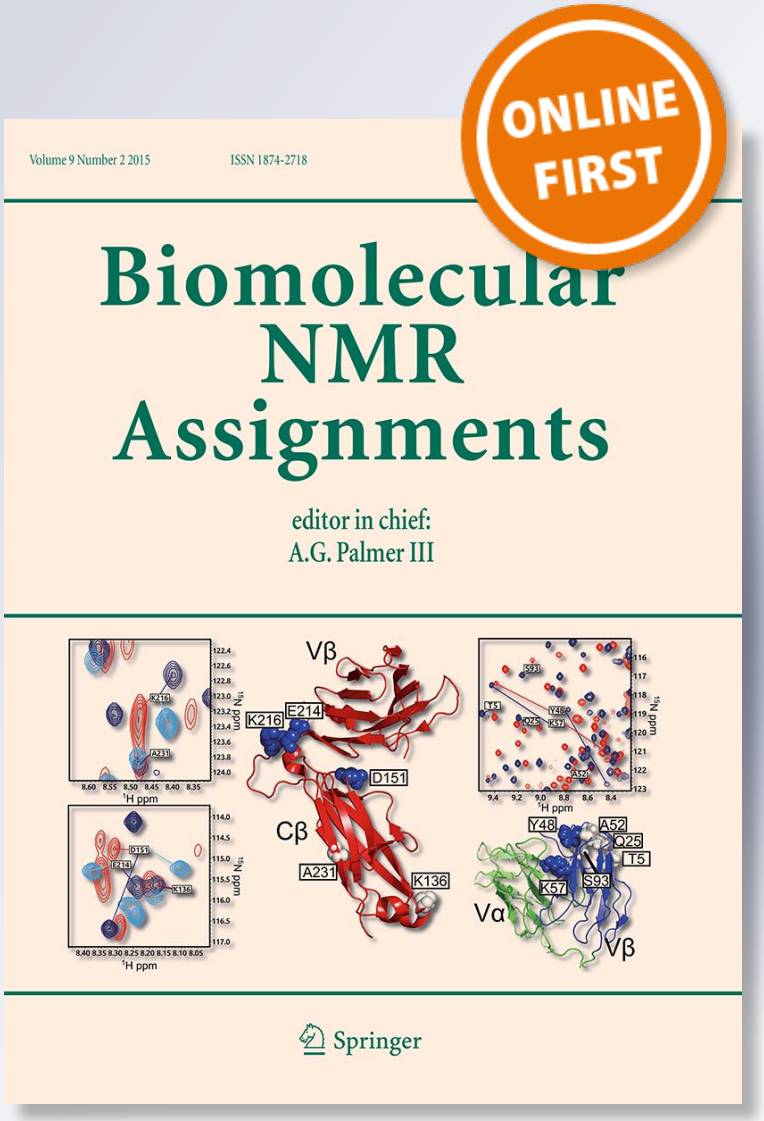

Springer

Biomolecular NMR Assignments
https://doi.org/10.1007/s12104-019-09915-9

ARTICLE

^{1}H, ^{13}C, and ^{15}N backbone and side chain chemical shift assignment of YdaS, a monomeric member of the HigA family

Maruša Prolič-Kalinšek[1,2] · Pieter De Bruyn[1,2] · Dukas Jurėnas[3] · Laurence Van Melderen[3] · Remy Loris[1,2] · Alexander N. Volkov[1,2,4]

Received: 12 July 2019 / Accepted: 3 October 2019

Abstract
The cryptic prophage CP-933P in *Escherichia coli* O157:H7 contains a *parDE*-like toxin–antitoxin module, the operator region of which is recognized by two flanking transcription regulators: PaaR2 (ParE associated Regulator), which forms part of the *paaR2-paaA2-parE2* toxin–antitoxin operon and YdaS (COG4197), which is encoded in the opposite direction but shares the operator. Here we report the ^{1}H, ^{15}N and ^{13}C backbone and side chain chemical shift assignments of YdaS from *Escherichia coli* O157:H7 in its free state. YdaS is a distinct relative to HigA antitoxins but behaves as a monomer in solution. The BMRB Accession Number is 27917.

Keywords Toxin–antitoxin module · DNA binding · Transcription regulation · Macromolecular structure

Biological context

Toxin–antitoxin (TA) modules are small operons involved in the stress response of bacteria and archaea. Six different types of TA modules have been identified based on the nature and mechanism of action of the antitoxin (for a review see Page and Peti 2016). The most common type, type II, encodes a protein toxin that is directly inhibited by a cognate protein antitoxin. Activation of the toxin involves proteolytic degradation of the antitoxin (for a review see Muthuramalingam et al. 2016) and leads to inhibition of cell growth (Pedersen et al. 2002) and, in case of prolonged activation, cell death (Amitai et al. 2004).

The physiological role of TA modules remains controversial. They were initially discovered on plasmids where they contribute to plasmid stability (Ogura and Hiraga 1983; Gerdes et al. 1986). The majority of TA modules are, however, located on chromosomes, where they have been proposed to serve as stress-response elements (Christensen et al. 2001), mediators of altruistic cell death (Erental et al. 2014) and/or mediators of persistence (Helaine et al. 2014), although the latter is being debated (Goormaghtigh et al. 2018). Other proposed functions include anti-addiction modules for plasmids (Saavedra De Bast et al. 2008), protection against bacteriophages (Hazan and Engelberg-Kulka 2004; Otsuka and Yonesaki 2012), selfish genes (Magnuson 2007) and the stabilization of genomic parasites such as conjugative transposons and temperate bacteriophages (Rowe-Magnus et al. 2003; Dziewit et al. 2007; Bustamante et al. 2014; Iqbal et al. 2015).

In line with the latter, the *paaR2-paaA2-parE2* operon, which encodes a ParE-like toxin ParE2, the corresponding antitoxin PaaA2 and a regulator PaaR2, is located in the cryptic prophage CP-933P in the genome of *Escherichia coli* O157:H7 (Hallez et al. 2010). The antitoxin PaaA2 is an intrinsically disordered protein without DNA-binding function (Sterckx et al. 2014), which wraps around ParE2 and sequesters the latter in a hetero-hexadecameric complex (Sterckx et al. 2016). PaaR2 represses transcription of the *paaR2-paaA2-parE2* operon by binding to the operator region (Hallez et al. 2010; De Bruyn et al. 2019). The open reading frame of another regulator, COG4197, is found upstream of this operator, but is transcribed in the opposite

✉ Remy Loris
remy.loris@vub.be

1 Structural Biology Brussels, Department of Biotechnology (DBIT), Vrije Universiteit Brussel, Brussels, Belgium

2 VIB-VUB Center for Structural Biology, Brussels, Belgium

3 Cellular and Molecular Microbiology, Department of Molecular Biology, Université Libre de Bruxelles, Gosselies, Belgium

4 Jean Jeener NMR Centre, Vrije Universiteit Brussel, Brussels, Belgium

Published online: 17 October 2019

sense relative to *paaR2-paaA2-parE2*. COG4197 contains a helix-turn-helix motif and competes with PaaR2 for the same operator region, thus adding another dimension to the regulation of the *paaR2-paaA2-parE2* TA operon (our unpublished results).

Sequence analysis shows that COG4197 is a homologue of YdaS, a transcription factor found in the cryptic prophage Rac of *E. coli* K12 and for which no structural data are available (Casjens 2003; Jobling 2018) and more distantly of the HigA antitoxin from *Pseudomonas putida* (see results). We will therefore refer to COG4197 as YdaS.

Currently, three types of HigA antitoxins are known. The first type, represented by *Vibrio cholerae* HigA, contains a folded C-terminal regulatory helix-turn-helix domain that is preceded by an intrinsically disordered N-terminal domain responsible for toxin neutralization (Hadži et al. 2017). The second type, represented by HigA proteins from *Proteus vulgaris* plasmid Rts1 (Schureck et al. 2014) and *Pseudomonas putida* (Talavera et al. 2019), is a fully folded single helix-turn-helix domain protein that combines both DNA binding and toxin-neutralizing functions. The third type, as exemplified by members found in *E. coli* and *Shigella flexneri*, has two distinct globular domains: an N-terminal dimerization domain and a C-terminal HTH domain that are connected by a long α-helix (Yang et al. 2016). All three types form obligate dimers, similar to all other known antitoxins that act as transcription regulators (for a review see Loris and Garcia-Pino 2014).

Here we describe the expression, purification and NMR ^{1}H, ^{13}C, and ^{15}N backbone and side chain chemical shift assignment of YdaS. We show that, contrary to expectation, YdaS behaves as a monomer and contains an intrinsically disordered region at its C-terminus. This makes it the representative of a fourth yet uncharacterized class of HigA proteins.

Methods and experiments

Protein expression and purification

The open reading frame of COG4197 from *E. coli* O157:H7 was cloned in a pET28b vector in the *Nco*I and *Not*I sites, providing a C-terminal His-tag (GSSHHHHHH) on COG4197. This plasmid was transformed into competent BL21 (DE3) cells. Transformed cells were plated on agar plates supplemented with kanamycin (25 µg/ml) and incubated at 37 °C overnight. LB medium supplemented with kanamycin (25 µg/ml) was inoculated with one colony and left incubating overnight at 37 °C while shaking at 130 rpm. Two ml of the overnight culture was added to 500 ml of minimal medium and incubated at 37 °C with shaking at 130 rpm. Minimal medium contained 6.79 g/l Na_2HPO_4, 3 g/l KH_2PO_4 and 1 g/l NaCl, 2 mM $MgSO_4$, 0.2 mM $CaCl_2$, 5 ml of BME vitamin mix (Sigma), 60 mg/l $FeSO_4{\cdot}7H_2O$, 12 mg/l $MnCl_2{\cdot}4H_2O$, 8 mg/l $CoCl_2{\cdot}6H_2O$, 7 mg/l $ZnSO_4{\cdot}7H_2O$, 3 mg/l $CuSO_4{\cdot}5H_2O$, 0.2 mg/l H_3BO_3, 50 mg/l EDTA, 2 g/l ^{13}C-glucose, 1 g/l $^{15}NH_4Cl$ and 25 µg/ml kanamycin. When the OD_{600} reached 0.6–0.8 the protein expression was induced with 0.5 mM isopropyl β-D-thiogalactopyranoside (IPTG). Upon induction the cultures were incubated overnight at 20 °C and then centrifugated at 5000 rpm for 15 min, resuspended in lysis buffer (20 mM Tris, 500 mM NaCl, 20 mM $MgCl_2$, pH 8.0, 0.1 mg/ml 4-(2-Aminoethyl)benzenesulfonyl fluoride hydrochloride (AEBSF) and 1 µg/ml leupeptine) and stored at −80 °C. To purify the protein, the frozen cells were thawed and DNaseI was added (50 µg/ml). The suspension was stirred for 30 min at 4 °C. The cells were lysed by sonication (three times for 1 min, 5 s on and 5 s off, 60% amplitude) and the lysate was centrifuged at 18,000 rpm for 45 min. The supernatant was then filtered (0.45 µm HAWP filter) and loaded onto a pre-packed HisTrap HP Ni^{2+}-Sepharose column (GE Healthcare), pre-equilibrated in 20 mM Tris-HCl, 500 mM NaCl, 5 mM imidazole, pH 8.0. The column was then washed with the same buffer until the baseline stabilization. A linear gradient (0.0–1.0 M imidazole in 20 column volumes) elution was applied using 20 mM Tris-HCl, 500 mM NaCl, 1M imidazole, pH 8.0. Fractions containing the protein were concentrated and loaded on a Superdex 75 16/60 SEC column (GE Healthcare) pre-equilibrated in 20 mM Tris-HCl, 500 mM NaCl, pH 8.0. The purity of the protein was assessed by SDS-PAGE. For NMR experiments, the protein was dialyzed against 20 mM sodium phosphate,150 mM NaCl, pH 6.0 and spun down at 13,300 rpm for 10 min prior to the measurements.

Analytical size exclusion chromatography

The purified protein YdaS was dialysed against 20 mM sodium phosphate, 150 mM NaCl, pH 6.0 and 100 µl was injected at a concentration of 1 mg/ml (84 µM) into BioRad EnRich SEC 70 HR 10 × 300 column, pre-equilibrated in the same buffer. The protein was eluted at the flow rate of 1 ml/min. A BioRad standard (50 µl) containing bovine thyroglobulin (670 kDa), bovine γ-globulin (158 kDa), chicken ovalbumin (44 kDa), horse myoglobin (17 kDa) and vitamin B12 (1.35 kDa) was injected and eluted under the same conditions as YdaS. The molecular mass and the radius of hydration were determined according to Uversky (1993).

Nuclear magnetic resonance (NMR) spectroscopy

The NMR sample contained 1 mM U-[^{13}C,^{15}N] YdaS in 20 mM sodium phosphate 150 mM NaCl pH 6.0 and 10% D_2O for the lock. All NMR spectra were acquired at 298 K on

a Bruker Avance III HD 800 MHz spectrometer, equipped with a TCI cryoprobe. The experimental set comprised 2D heteronuclear single quantum correlation spectra (^{1}H,^{15}N-HSQC and ^{1}H,^{13}C-HSQC), 3D ^{15}N- and ^{13}C-NOESY-HSQC (mixing times of 120 ms), triple-resonance BEST-HNCACB, BEST-HN(CO)CACB, BEST-HNCO, BEST-HN(CA)CO, HBHA(CO)NH, (H)CCH-TOCSY, and H(C)CH-TOCSY (Sattler et al. 1999) and 2D (HB)CB(CGCD)HD and (HB)CB(CGCDCE)HE for the assignment of aromatic residues (Yamazaki et al. 1993). All 3D experiments were acquired with a non-uniform sampling (20–50%) as implemented in TopSpin 3.5 (Bruker). The NMR data were processed in TopSpin 3.5 (Bruker) or MddNMR (Orekhov and Jaravine 2011) and NMRPipe (Delaglio et al. 1995), and analyzed in CCPNMR (Vranken et al. 2005).

Assignment and data deposition

Semi-automatic assignment of the protein backbone was performed in CCPNMR (Vranken et al. 2005). The assignments of N, NH, Hα, Hβ, CO, Cα, and Cβ atoms were obtained from the identification of intra- and inter-residue connectivities in HNCACB, HN(CO)CACB, HNCO, HN(CA)CO, and HBHA(CO)HN spectra at the ^{1}H,^{15}N frequencies of every peak in the ^{1}H,^{15}N-HSQC spectrum. Assignments were extended to the side chain signals using correlations within (H)CCH-TOCSY, H(C)CH-TOCSY, (HB)CB(CGCD)HD and (HB)CB(CGCDCE)HE experiments. Remaining aromatic ^{1}H and ^{13}C assignments were obtained from constant-time ^{1}H,^{13}C-HSQC and ^{13}C-NOESY-HSQC spectra, focused on the aromatic region. Side-chain NH_2 groups of glutamines and Hε atoms of methionines were assigned from 3D ^{15}N- and ^{13}C-NOESY-HSQC spectra. Finally, all ^{1}H, ^{13}C and ^{15}N resonances were verified by 3D ^{15}N- and ^{13}C-NOESY-HSQC experiments.

YdaS was expressed in *E. coli* BL21 (DE3) and purified to homogeneity. The protein migrates on SDS-PAGE as a band of an apparent molecular weight of 14 kDa, in close agreement with the theoretical mass of 11,902.3 Da as calculated from its amino acid sequence. Analytical SEC shows a single peak eluting at 12.50 ml (Fig. 1), which corresponds to a radius of hydration (R_H) of 1.53 nm and an estimated molecular weight of 17.5 kDa. The larger molecular weight determined by SEC compared to the theoretical one indicates a non-spherical shape or an intrinsically disordered C-tail, but still indicates that YdaS is a monomer rather than a dimer.

The ^{1}H,^{15}N-HSQC spectrum of YdaS features a complete set of well-resolved resonances, typical for a folded protein (Fig. 2). Excluding the C-terminal hexa-histidine tag, 99% of all backbone and 96% of all ^{1}H side-chain resonances were assigned. The backbone amide of Asp14, Cγ/Hγ and Cδ/Hδ groups of Pro41, Cγ/Hγ atoms of Glu48,

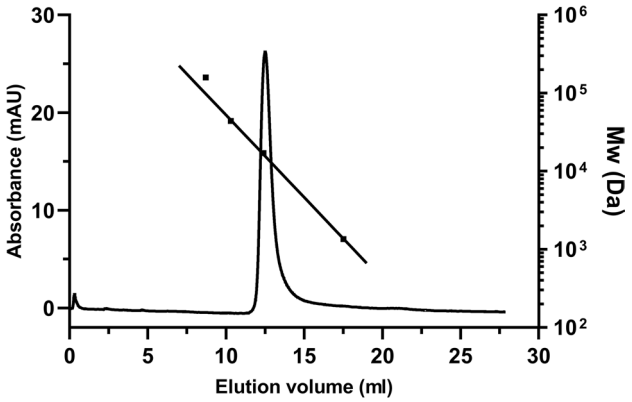

Fig. 1 Elution profile of YdaS (84 µM) on a BioRad EnRich SEC 70 HR 10×300 column shown together with elution volumes of protein standards (squares). These MW standards were fitted according to Uversky (1993). The molecular weight of bovine thyroglobulin (670 kDa) falls outside the linear range of this column and was therefore not taken into account in the fit

and Cγ/Hγ and Cδ/Hδ atoms of Arg57 were not observed in the spectra. In addition, the aromatic resonances of histidine residues 63, 82, and 85 could not be unambiguously assigned because of a strong spectral overlap with the signals of the hexahistidine tag. The ^{1}H, ^{13}C and ^{15}N chemical shifts for YdaS have been deposited in the BioMagResBank (http://www.bmrb.wisc.edu/) under the Accession Number 27917.

Predicted from the backbone chemical shifts using the chemical shift index (CSI) function and the DANGLE module (Cheung et al. 2010) in CCPNMR, the secondary structure of YdaS consists of five short α-helices, followed by a tail that contains several isolated residues with a high propensity for β-strand. There is, however, only a single such stretch (residues 80–90) that contains three residues, which indicates that likely no real β-sheet is formed and that the C-terminal tail lacks regular secondary structure (Fig. 3).

This secondary structure is consistent with those of homologues of YdaS being annotated in the UniProt data bank (The UniProt Consortium 2019) as YdaS-like and/or HigA-like proteins belonging to the Cro repressor superfamily. Indeed, a BLAST search of YdaS against the Protein Data Bank identifies GraA from *Pseudomonas putida*, a HigA family member as the closest homolog, although sequence identity is weak (11%) and concentrated in the HTH core. Compared to GraA and other HigA proteins, the presence of a C-terminal intrinsically disordered region is unique for YdaS. While this is a common feature of many TA antitoxins, the HigA family represented by *Proteus vulgaris* HigA and *Pseudomonas putida* GraA does not carry such a region (Schureck et al. 2014; Talavera et al. 2019). Therefore, YdaS appears to represent a novel family within the HigA superfamily, although it is not directly part of a toxin–antitoxin

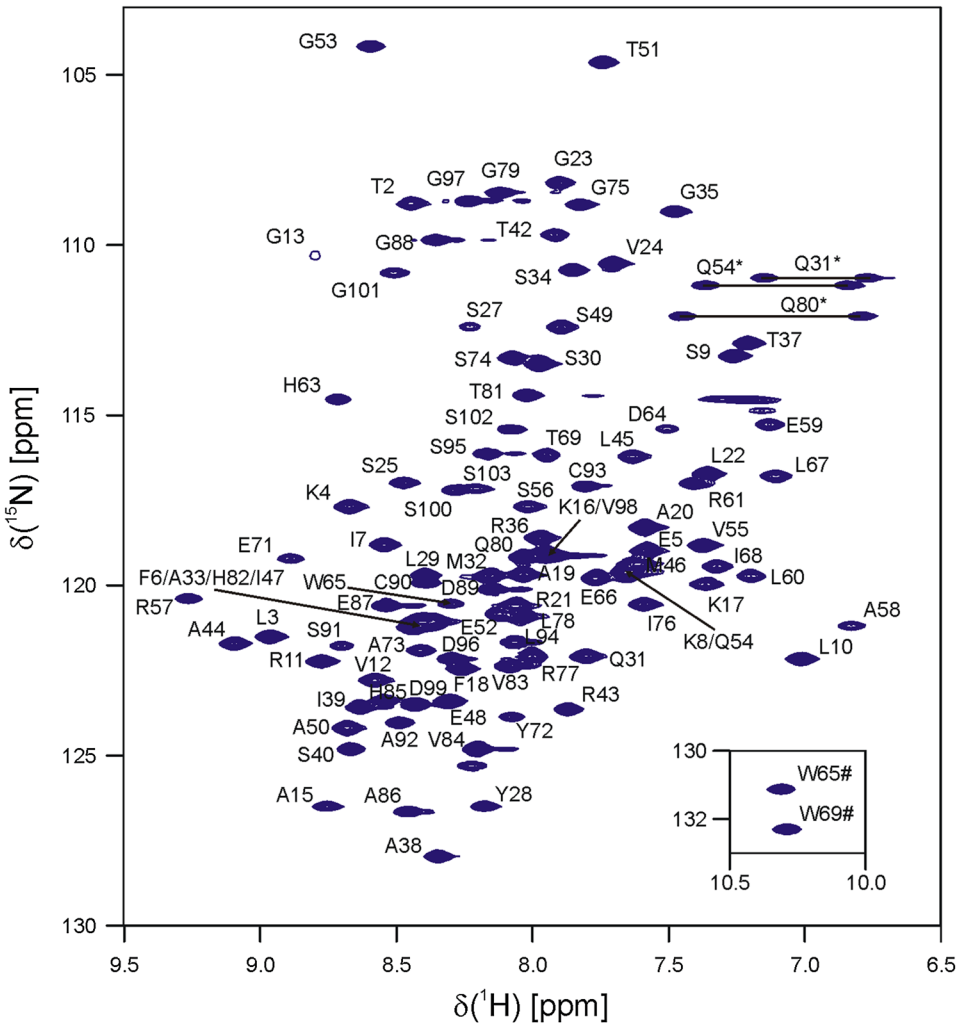

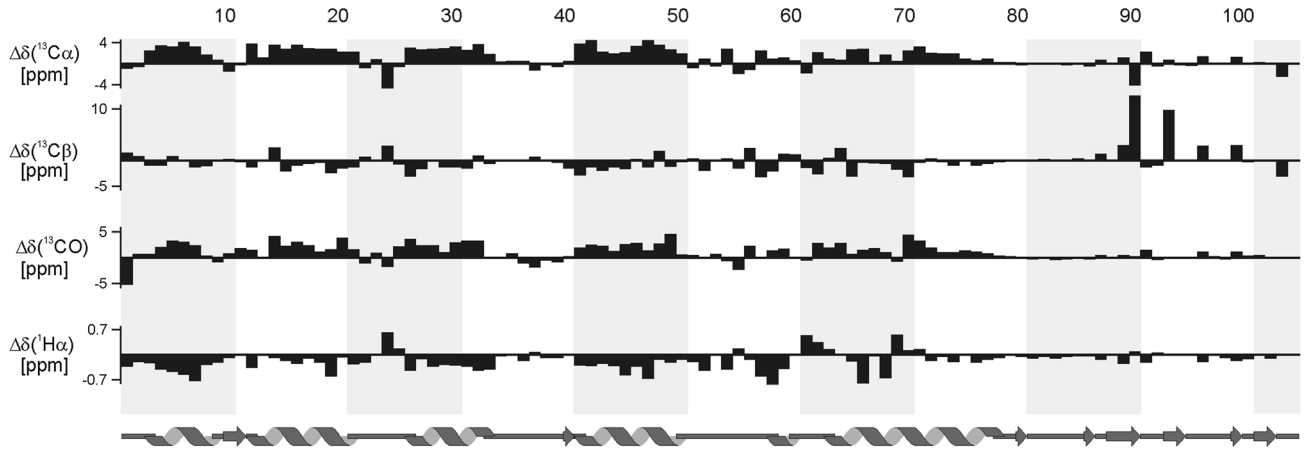

Fig. 2 Assigned [^{1}H,^{15}N]-HSQC spectrum of YdaS in 20 mM sodium phosphate 150 mM NaCl pH 6.0 and 10% D_2O, annotated with the assignments of the backbone amides and Gln side-chain NH_2 groups (joined by horizontal lines and labelled by asterisks). Indole amide resonances of W65 and W69 (labelled by hash symbols) are shown in the inset

Fig. 3 Secondary structure prediction of YdaS. Threshold deviations from random-coil ^{13}Cα, ^{13}Cβ, ^{13}CO, and ^{1}Hα chemical shifts are plotted as a function of the YdaS residue number using the chemical shift index (CSI) module in CCPNMR. The secondary structure of YdaS is shown in cartoon (predicted by the CSI and DANGLE modules in CCPNMR)

system as such (Christensen-Dalsgaard et al. 2010; Jobling 2018).

Acknowledgements This work received financial support from FWO-Vlaanderen (project nr. (G.0226.17N) and the Onderzoeksfonds of the Vrije Universiteit Brussel (OZR-VUB, Grant SPR13).

References

Amitai S, Yassin Y, Engelberg-Kulka H (2004) MazF-mediated cell death in *Escherichia coli*: a point of no return. J Bacteriol 186:8295–8300

Bustamante P, Tello M, Orellana O (2014) Toxin–antitoxin systems in the mobile genome of *Acidithiobacillus ferrooxidans*. PLoS ONE 9:e112226

Casjens S (2003) Prophages and bacterial genomics: what have we learned so far? Mol Microbiol 49:277–300

Cheung MS, Maguire ML, Stevens TJ, Broadhurst RW (2010) DANGLE: A Bayesian inferential method for predicting protein backbone dihedral angles and secondary structure. J Magn Reson 202:223–233

Christensen SK, Mikkelsen M, Pedersen K, Gerdes K (2001) RelE, a global inhibitor of translation, is activated during nutritional stress. Proc Natl Acad Sci USA 98:14328–14333

Christensen-Dalsgaard M, Jørgensen MG, Gerdes K (2010) Three new RelE-homologous mRNA interferases of *Escherichia coli* differentially induced by environmental stresses. Mol Microbiol 75:333–348

De Bruyn P, Hadži S, Vandervelde A, Konijnenberg A, Prolič-Kalinšek M, Sterckx YG, Sobott F, Lah J, Van Melderen L, Loris R (2019) Thermodynamic stability of the transcription regulator PaaR2 from *Escherichia coli* O157:H7. Biophys J 116:1420–1431

Delaglio F, Grzesiek S, Vuister GW, Zhu G, Pfiefer J, Bax A (1995) NMRPipe: a multidimensional spectral processing system based on UNIX pipes. J Biomol NMR 6:277–293

Dziewit L, Jazurek M, Drewniak L, Baj J, Bartosik D (2007) The SXT conjugative element and linear prophage N15 encode toxin–antitoxin-stabilizing systems homologous to the tad-ata module of the *Paracoccus aminophilus* plasmid pAMI2. J Bacteriol 189:1983–1997

Erental A, Kalderon Z, Saada A, Smith Y, Engelberg-Kulka H (2014) Apoptosis-like death, an extreme SOS response in *Escherichia coli*. MBio 5:e01426–e01414

Gerdes K, Rasmussen PB, Molin S (1986) Unique type of plasmid maintenance function: postsegregational killing of plasmid-free cells. Proc Natl Acad Sci USA 83:3116–3120

Goormaghtigh F, Fraikin N, Putrinš M, Hallaert T, Hauryliuk V, Garcia-Pino A, Sjödin A, Kasvandik S, Udekwu K, Tenson T, Kaldalu N, Van Melderen L (2018) Reassessing the role of type II toxin–antitoxin systems in formation of *Escherichia coli* Type II persister cells. MBio 9:e00640–e00618

Hadži S, Garcia-Pino A, Haesaerts S, Jurenas D, Gerdes K, Lah J, Loris R (2017) Ribosome-dependent *Vibrio cholerae* mRNAse HigB2 is regulated by a β-strand sliding mechanism. Nucleic Acids Res 45:4972–4983

Hallez R, Geeraerts D, Sterckx Y, Mine N, Loris R, Van Melderen L (2010) New toxins homologous to ParE belonging to three-component toxin–antitoxin systems in *Escherichia coli* O157:H7. Mol Microbiol 76:719–732

Hazan R, Engelberg-Kulka H (2004) *Escherichia coli* mazEF-mediated cell death as a defense mechanism that inhibits the spread of phage P1. Mol Genet Genomics 272:227–234

Helaine S, Cheverton AM, Watson KG, Faure LM, Matthews SA, Holden DW (2014) Internalization of *Salmonella* by macrophages induces formation of nonreplicating persisters. Science 343:204–208

Iqbal N, Guérout A-M, Krin E, Le Roux F, Mazel D (2015) Comprehensive functional analysis of the 18 *Vibrio cholerae* N16961 toxin–antitoxin systems substantiates their role in stabilizing the superintegron. J Bacteriol 197:2150–2159

Jobling MG (2018) Ectopic expression of the *ydaS* and *ydaT* genes of the cryptic prophage Rac of *Escherichia coli*. K-12 may be toxic but do they really encode toxins?: a case for using genetic context to understand function. mSphere 3:e00163–e00118

Loris R, Garcia-Pino A (2014) Disorder- and dynamics-based regulatory mechanisms in toxin–antitoxin modules. Chem Rev 114:6933–6947

Magnuson RD (2007) Hypothetical functions of toxin–antitoxin systems. J Bacteriol 189:6089–6092

Muthuramalingam M, White JC, Bourne CR (2016) Toxin–antitoxin modules are pliable switches activated by multiple protease pathways. Toxins 8:E214

Ogura T, Hiraga S (1983) Mini-F plasmid genes that couple host cell division to plasmid proliferation. Proc Natl Acad Sci USA 80:4784–4788

Orekhov VV, Jaravine VA (2011) Analysis of non-uniformly sampled spectra with multi-dimensional decomposition. Prog Nucl Magn Reson Spectrosc 59:271–292

Otsuka Y, Yonesaki T (2012) Dmd of bacteriophage T4 functions as an antitoxin against *Escherichia coli* LsoA and RnlA toxins. Mol Microbiol 83:669–681

Page R, Peti W (2016) Toxin–antitoxin systems in bacterial growth arrest and persistence. Nat Chem Biol 12:208–214

Pedersen K, Christensen SK, Gerdes K (2002) Rapid induction and reversal of a bacteriostatic condition by controlled expression of toxins and antitoxins. Mol Microbiol 45:501–510

Rowe-Magnus DA, Guerout AM, Biskri L, Bouige P, Mazel D (2003) Comparative analysis of superintegrons: engineering extensive genetic diversity in the *Vibrionaceae*. Genome Res 13:428–442

Saavedra De Bast MS, Mine N, Van Melderen L (2008) Chromosomal toxin–antitoxin systems may act as antiaddiction modules. J Bacteriol 190:4603–4609

Sattler M, Schleucher J, Griesinger C (1999) Heteronuclear multidimensional NMR experiments for the structure determination of proteins in solution employing pulsed field gradients. Prog Nucl Magn Reson Spectrosc 34:93–158

Schureck MA, Maehigashi T, Miles SJ, Marquez J, Cho SE, Erdman R, Dunham CM (2014) Structure of the *Proteus vulgaris* HigB-(HigA)$_2$-HigB toxin–antitoxin complex. J Biol Chem 289:1060–1070

Sterckx YG, Volkov AN, Vranken WF, Kragelj J, Jensen MR, Buts L, Garcia-Pino A, Jové T, Van Melderen L, Blackledge M, van Nuland NA, Loris R (2014) Small-angle X-ray scattering- and nuclear magnetic resonance-derived conformational ensemble of the highly flexible antitoxin PaaA2. Structure 22:854–865

Sterckx YG, Jové T, Shkumatov AV, Garcia-Pino A, Geerts L, De Kerpel M, Lah J, De Greve H, Van Melderen L, Loris R (2016) A unique hetero-hexadecameric architecture displayed by the *Escherichia coli* O157 PaaA2-ParE2 antitoxin–toxin complex. J Mol Biol 428:1589–1603

Talavera A, Tamman H, Ainelo A, Konijnenberg A, Hadži S, Sobott F, Garcia-Pino A, Hõrak R, Loris R (2019) A dual role in regulation and toxicity for the disordered N-terminus of the toxin GraT. Nat Commun 10:972

The UniProt Consortium (2019) UniProt: a worldwide hub of protein knowledge. Nucleic Acids Res 47:D506–D515

Uversky VN (1993) Use of fast protein size-exclusion liquid chromatography to study the unfolding of proteins which denature through the molten globule. Biochemistry 32:13288–13298

Vranken WF, Boucher W, Stevens TJ, Fogh RH, Pajon A, Llinas M, Ulrich EL, Markley JL, Ionides J, Laue ED (2005) The CCPN data model for NMR spectroscopy: development of a software pipeline. Proteins 59:687–696

Yamazaki T, Forman-Kay JD, Kay LE (1993) Two-dimensional NMR experiments for correlating 13Cb and 1Hd/e chemical shifts of aromatic residues in 13C-labeled proteins via scalar couplings. J Am Chem Soc 115:11054–11055

Yang J, Zhou K, Liu P, Dong Y, Gao Z, Zhang J, Liu Q (2016) Structural insight into the *E. coli* HigBA complex. Biochem Biophys Res Commun 478:1521–1527